Digest Journal of Nanomaterials and Biostructures Vol. 12, No. 2, April - June 2017, p. 431 - 440

CELL ADHESION AND ALIGNMENT OF HUMAN OSTEOBLASTS AND HUMAN GINGIVAL FIBROBLASTS ON MICRO/NANO-GROOVED GELATIN SHEET

N. KAGA[a*], T. AKASAKA[b], R. HORIUCHI[a], Y. YOSHIDA[b], A. YOKOYAMA[a]
[a]*Department of Oral Functional Prosthodontics, Hokkaido University Graduate School of Dental Medicine, Sapporo 060-8586, Japan*
[b]*Department of Biomedical Materials and Engineering, Hokkaido University Graduate School of Dental Medicine, Sapporo 060-8586, Japan*

We investigated the influence of micro/nano-grooved gelatin sheets on human osteoblasts (NHOst) and human gingival fibroblasts (HGF) for implant surface engineering purposes. We prepared grooved gelatin sheets with widths of 500 nm, 1 μm, and 2 μm via nano-imprinting and thermal crosslinking. We then compared the adhesion behavior and alignment of NHOst and HGF on the grooved gelatin sheets *in vitro*. The number of attached cells on the grooved gelatin sheets was about 1.5-1.7 times higher than that of those on the plane gelatin sheets (control) for both cell types. Furthermore, both cell types exhibited strong contact guidance and clear alignment along the gelatin groove direction. These results suggest that both cell types were easily attached and aligned on the grooved-gelatin sheets because our patterns have adequate groove widths and because both cell types have good cell alignment capability.

(Received April 3, 2017; Accepted May 20, 2017)

Keywords: Gelatin sheet; Human gingival fibroblasts; Human osteoblasts; Micro/nano-pattern; Thermal crosslinking

1. Introduction

Dental implants are widely used to clinically replace missing teeth in the mandible and/or maxilla. After implant insertion, the implant surface attaches to the gingiva, restricting bacterial invasion. Subsequently, the implant surface achieves osseointegration by direct contact with living bone. However, infection is known as one of the risk factors for the failure of dental implants [1,2].

Inflammation around implants is called peri-implantitis; it has attracted attention as a complicated problem that is difficult to resolve. Peri-implantitis is an inflammatory process that irritates tissues around the implant and causes bone loss, leading to failure of the dental implant [3,4]. Many types of research have focused on peri-implantitis prevention to ensure implant success. Nevertheless, unexpected cases after treatment are sometimes reported in which the infection invades the complex surface of the implant, followed by bone resorption around the implant [1, 5]. Therefore, re-osseointegration or bone regeneration is extremely unlikely at the implant body.

Many therapeutic or preventive approaches against peri-implantitis have been reported [5]. For the prevention of peri-implantitis through biomaterials, anti-bioadhesion coatings or antimicrobial releasing coatings have been developed. Alternatively, the development of a stable permucosal seal around the implant may be the simplest long-term protection from peri-implantitis and bone resorption. Titanium surfaces with specific microgroove textured patterns, *e.g.*, Laser-Lok implants (BioHorizons, Atlanta, GA, USA), promote the attachment and organization of osteoblasts and fibroblasts, leading to greater osseointegration or effective soft-tissue attachment [6, 7]. Furthermore, nano-textured grooves on the titanium implant surface can improve bone

*Corresponding author: n.kaga@den.hokudai.ac.jp

tissue and implant interface interactions by stimulating osteoblast adhesion, proliferation, and differentiation [8]. Therefore, implant surfaces with effective micro/nano-textured designs are expected to attach rapidly and strongly to osteoblasts and gingival fibroblasts for peri-implantitis prevention.

Collagen and gelatin have been used as coating agents for dental implants to positively interact with peri-implant tissues. Collagen is a major component of connective tissue in the body [9], and gelatin is denatured collagen. Collagen/gelatin components have been previously immobilized on the surface of implants by dip-coating [10], silanization [11], and electrospray deposition [12]. The effects of collagen/gelatin coatings are expected to enhance initial cell attachment and proliferation and subsequently improve the attachment of the peri-implant soft tissue and/or enhance osseointegration.

For the control of cell adhesion and function, patterned collagen/gelatin coatings have recently been fabricated by the following methods: polymerization of methacrylated gelatin [13], coating on patterned substrates [14], self-assembly of collagen fibers [15], and crosslinking [16-24] in combination with micro/nano-molding, 3D printing, photo-masking, *etc*. Although the patterns of collagen/gelatin have been fabricated in the micro- to nano-scale range, smaller patterns are difficult to be fabricated because of the weakness and solubility of collagen/gelatin substances. Many studies have chosen crosslinking approaches for patterned collagen/gelatin coatings using glutaraldehyde [16], formaldehyde [17], carbodiimide [18], genipin [19], riboflavin [20], transglutaminase [21], silane coupling agent [22], and thermal dehydration [23, 24].

Li *et al*. reported that nano-patterned gelatin was fabricated by crosslinking with 10% formaldehyde [17]. NIH/3T3 cells on nano-grooves of 400 nm pitch demonstrated strong cell elongation and faster cell adhesion. Zorlutuna *et al*. reported that nano-patterned collagen films were fabricated by crosslinking with carbodiimide [18]. However, the nano-grooves between widths of 333 nm and 650 nm did not affect endothelial cell proliferation and initial cell alignment. These findings indicate that cell type and pattern size can influence the efficiency of cell adhesion and alignment. In addition, the type of substrate materials or crosslinking agents could potentially influence cell behavior. However, there are limited reports of cell adhesion and alignment with patterns of collagen/gelatin that range in size from micro- to nano-scales. Cells associated with the peri-implant tissue, such as human osteoblasts (NHOst) or human gingival fibroblasts (HGF), have not been investigated for compatibility with patterned collagen/gelatin coating.

In this study, we investigated the influence of micro/nano-patterned gelatin sheets on NHOst and HGF for implant surface engineering purposes. We prepared micro/nano-grooved gelatin sheets with widths of 500 nm to 2 μm and a depth of 500 nm via nano-imprinting and thermal crosslinking. Next, we compared the cell adhesion and alignment behaviors of both cell types on the patterned gelatin sheets *in vitro*.

2. Materials and Methods

2.1. Preparation of micro/nano-grooved gelatin sheets

Fig. 1 shows the procedure for fabrication of micro/nano-grooved gelatin sheets. A quartz master mold was purchased (Kyodo International Inc., Kawasaki, Japan). Three areas of 5×5 mm^2 used in this study were patterned with ridge widths of 500 nm, 1 μm, and 2 μm and a groove height or depth of 500 nm. A glycol-modified polyethylene terephthalate film (G-PET; Sawada Platec Co., Ltd., Saitama, Japan) was pressed on the master mold with 0.2 MPa at 105°C for 5 min using a thermal nanoimprint apparatus (AH-1TC; Shimadzu Corp., Kyoto, Japan), and it was gradually cooled down to 23°C. Subsequently, the film was carefully peeled off, and a replica G-PET mold was obtained (Fig. 2a). Gelatin powder from porcine skin (Sigma-Aldrich, Tokyo, Japan) was dissolved at a final concentration of 10 wt% in distilled water at 60°C. Then, 0.3 mL of the 10 wt% gelatin solution was dropped on the replica G-PET mold and dried for 24 h at 37°C. The dried gelatin sheet was carefully peeled off from the mold (Fig. 2b). The resulting patterned sheet was thermally crosslinked for 2 h at 200°C. The swollen gelatin sheet in H_2O was gently

transferred into a culture dish and adhered with a photopolymer paste (Biosurfine-AWP; Toyo Gosei Co., Ltd., Chiba, Japan) to the bottom of the dish (Fig. 2c). All sheets were sterilized under UV light for 30 min.

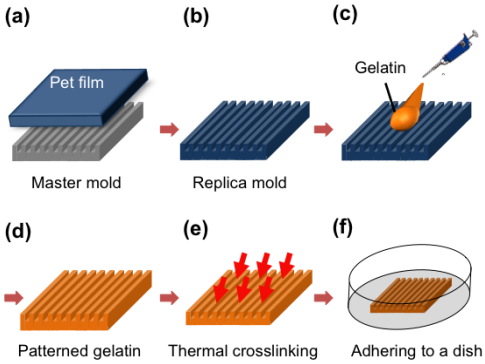

Fig. 1. Procedure for fabrication of micro/nano-patterned gelatin sheets. The procedure involved (a) setting the PET film on the micro/nano-patterned master mold, (b) peeling off the replica mold of patterned PET, (c) dropping of gelatin solution on the replica mold, (d) peeling off the patterned gelatin, (e) thermal crosslinking of the gelatin at 200°C for 2 h, and (f) adhering the patterned gelatin to a culture dish.

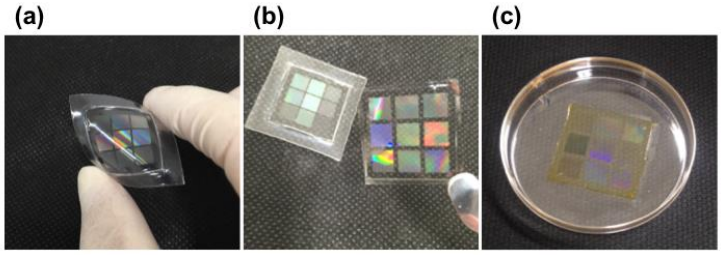

Fig. 2. Macroscopic view of the replica mold and the patterned gelatin sheet. (a) Replica mold with PET film. (b) Peeled patterned gelatin sheet. (c) Micro/nano-patterned gelatin sheet adhered on a culture dish.

2.2. Scanning electron microscope (SEM) and laser microscope observations

For SEM (S-4000; Hitachi High-Tech Fielding Corp., Tokyo, Japan) observation, the patterned gelatin sheets were sputter-coated with Pt-Pd by a sputtering apparatus (E-1030; Hitachi High-Tech Fielding Corp., Tokyo, Japan). Then, SEM images of the surface patterns were obtained (Fig. 3). Surface topography and line profile of the Pt-Pd-coated patterned gelatin sheets were measured with a 3D laser microscope (VK-X200; Keyence, Osaka, Japan) (Fig. 4).

2.3. Cell culture

NHOst (CC-2538; Lonza Japan, Tokyo, Japan) and HGF (cat. number 2620; Cosmo Bio Co., Ltd., Tokyo, Japan) were cultured in Dulbecco's modified Eagle's medium (DMEM; Sigma) supplemented with 10% fetal bovine serum (FBS; CELLect Silver from Mexico, MP Biomedicals Inc., Solon, OH, USA) in 1% penicillin-streptomycin-amphotericin B suspension (Wako Pure Chemical Industries, Ltd., Osaka, Japan). The cultured cells were incubated at 37°C in a humidified atmosphere of 5% CO_2 and 95% air. Cells were checked for growth every day, and the medium was exchanged twice a week. At 70% confluence, the cells were treated with a cell detachment reagent (Accumax^{TM}; Funakoshi Co., Ltd., Tokyo, Japan), and single floating cells were counted by a hemocytometer. Then, the cells were used in subsequent assays.

2.4. Cell adhesion and alignment

To investigate cell behavior on the patterned gelatin sheets, we performed a cell adhesion [25] and cell alignment assay [26]. The patterned gelatin sheet on each dish was immersed in

DMEM with 10% FBS in 1% penicillin-streptomycin-amphotericin B suspension. NHOst and HGF were seeded at a density of 5,000 cells/cm^2 on the patterned gelatin sheets and incubated at 37°C in a humidified atmosphere of 5% CO_2 and 95% air for 1 h to allow cell adhesion. During the experiment, the cells were fixed in 2.5% glutaraldehyde and stained with Giemsa staining solution. Cell adhesion and alignment were observed under an optical microscope (ECLIPSE E200; Nikon, Tokyo, Japan) equipped with a digital camera. Attached cell number (Fig. 5) and orientation angle (Fig. 6) were estimated on the photographs of each grooved gelatin pattern by the software ImageJ. Variations in the cell density were calculated from the half-field (2.5×2.5 mm^2/field) of each pattern. Error bars indicate a standard deviation of n=4 (Fig. 5). The cell orientation angles of 100 cells from each pattern were determined, and frequency distributions of the cell orientation angles were calculated (Fig. 6).

2.5. SEM observation of cell morphology

For SEM observation, the patterned gelatin sheets with 1-h adherent cells were rinsed with phosphate-buffered saline (PBS) to remove non-adherent cells, and they were fixed with 2.5% glutaraldehyde solution. Then, the patterned gelatin sheets were dehydrated sequentially in 50%, 60%, 70%, 80%, 90%, 95%, and 100% ethanol for 5 min each, followed by critical point drying at 37°C. The patterned gelatin sheets were sputter-coated with Pt-Pd for morphological examination with SEM.

2.6. Statistical analysis

Statistical analysis was performed using GraphPad Prism version 6.05 (GraphPad Software, Inc., La Jolla, CA, USA). All data are presented as the mean and standard deviation. Statistical differences were assessed by one-way ANOVA and Tukey's multiple comparison post-hoc test. A value of $p<0.05$ is considered statistically significant.

3. Results

3.1. Preparation of micro/nano-grooved gelatin sheets

The patterned gelatin sheets were prepared at the micro/nano level by nano-imprinting with gelatin solution and thermal crosslinking as illustrated in Fig. 1. Patterns on the gelatin sheet were easily molded according to the corresponding patterns of the replica G-PET mold during our replication process (Fig. 2a and b). After crosslinking, the patterned gelatin sheet was adhered on a culture dish (Fig. 2c). The patterned gelatin sheet adhered on each dish was stable during cell culture. Three out of the nine grooved patterns shown in the image were used for cell assays.

Surface SEM images of the resulting patterns after thermal crosslinking are shown in Fig. 3. Finely grooved structures were molded from the corresponding shape; the surface of the each pattern was smooth at the nano level. Patterns with widths of 500 nm, 1 μm, and 2 μm roughly maintained their ridges and grooves after thermal crosslinking. Fig. 4 shows the laser microscope and line profile image of a representative grooved gelatin sheet with 1 μm widths; finely grooved structures were observed both before and after thermal crosslinking. Based on line profile data, the gelatin pattern had 1 μm widths and 0.4 μm depths before thermal crosslinking, while the crosslinked gelatin pattern had 0.8 μm widths and 0.3 μm depths. As a result of dry conditions, both the widths and heights of the grooves after thermal crosslinking were reduced by about 80% compared with those of the grooves before thermal crosslinking.

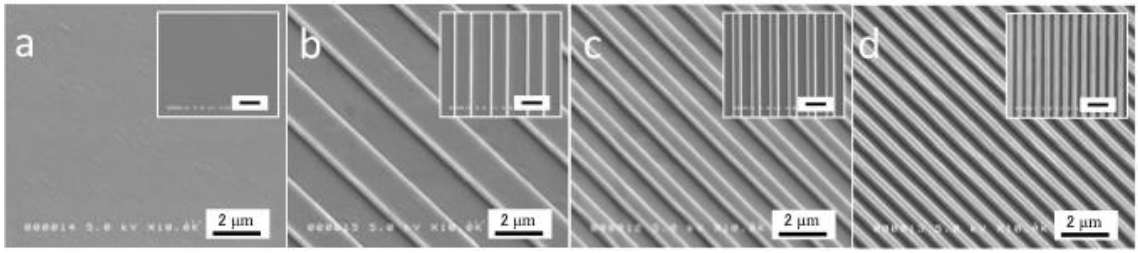

Fig. 3. SEM images of the patterned gelatin surface after thermal crosslinking at an angle of 45°. Inset shows a top view image of the pattern surface. (a) Plane (control). (b) 2 μm groove. (c) 1 μm groove. (d) 500 nm groove. Scale bars: 2 μm.

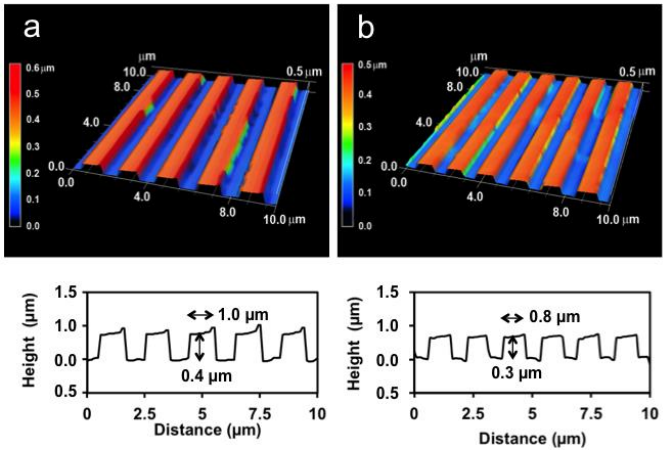

Fig. 4. Laser microscope images and line profiles of a representative grooved gelatin sheet with 1 μm widths (a) before and (b) after thermal crosslinking.

3.2. Cell adhesion and alignment

Fig. 5 shows the number of attached NHOst and HGF on the grooved gelatin sheets after 1 h. The number of attached cells on the grooved gelatin sheets was about 1.5-1.7 times higher than that of those on the plane gelatin sheets (control) (p<0.05) for both cell types. However, the number of attached cells of both cell types was not significantly different (p>0.05) among the 500 nm, 1 μm, and 2 μm grooved gelatin patterns.

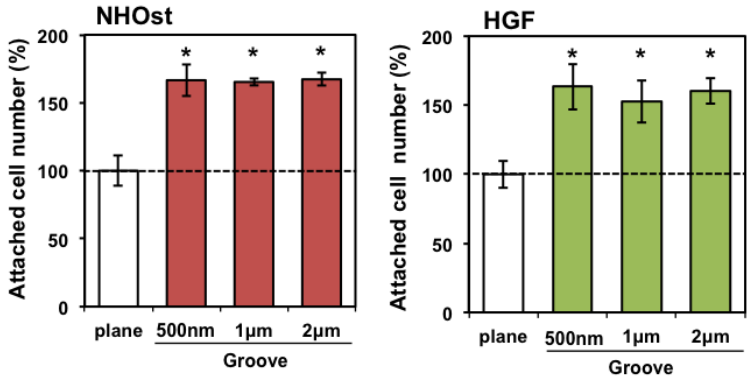

Fig. 5. The attached cell number of human osteoblasts (NHOst) and human gingival fibroblasts (HGF) on grooved gelatin sheets with groove widths of 500 nm, 1.0 μm, and 2.0 μm after 1 h incubation. The attached cell number was normalized to that of the plane gelatin sheet (control). The normalized value of the plane gelatin sheet was set as 100%. (indicates p<0.05).*

Fig. 6 shows the cell alignment of NHOst and HGF on plane gelatin sheets and 500 nm grooved gelatin sheets after 1 h incubation. The cell alignment of NHOst and HGF demonstrated no difference in morphology between the 500 nm, 1 μm, and 2 μm grooved gelatin sheets. Optical microscope images of both cell types on the plane and the grooved gelatin sheets are shown in Fig. 6a. After 1 h incubation, NHOst on the plane gelatin sheets were observed as large extended cells, whereas NHOst on the 500 nm grooved gelatin sheets were observed as large elongated cells. HGF showed a similar morphology as NHOst without exhibiting a smaller cell area. Frequency distributions of the cell orientation angles are shown in Fig. 6b. About 80% of both cell types were distributed between an orientation angle of 0° and 15° on the grooved gelatin sheets, whereas both cell types were randomly distributed on the plane gelatin sheets. On the gelatin grooves, both cell types exhibited strong contact guidance and clear alignment along the gelatin groove direction.

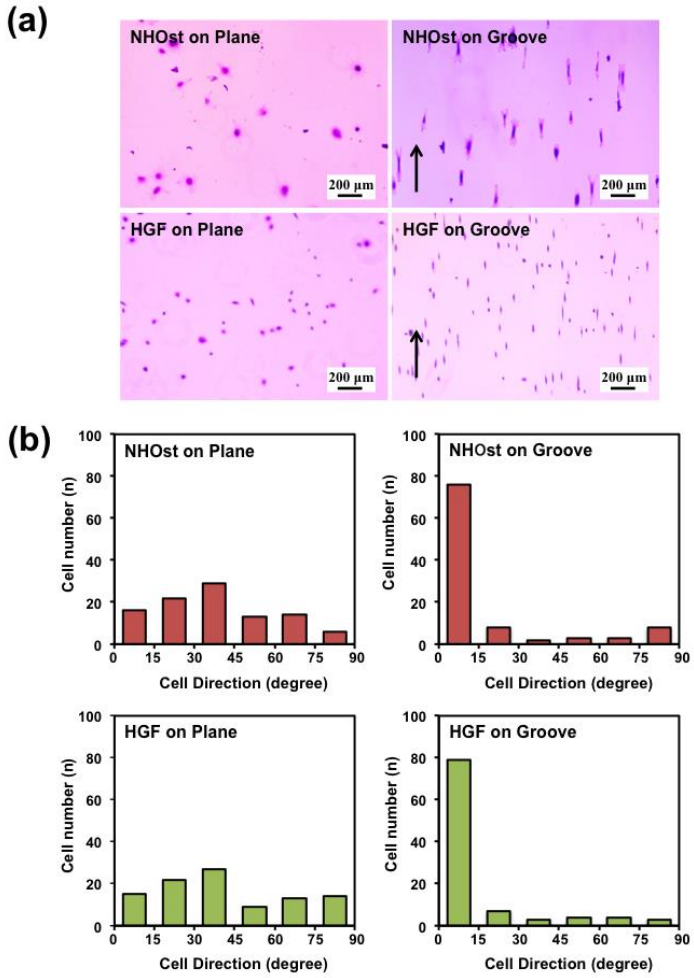

Fig. 6. Cell alignment of human osteoblasts (NHOst) and human gingival fibroblasts (HGF) on the 500 nm grooved gelatin sheet after 1 h incubation. (a) Optical microscope images of the stained cells. The arrow indicates groove direction. (b) Frequency distributions of the cell orientation angles (degrees).

Fig. 7 shows typical SEM images of attached NHOst and HGF on the plane gelatin sheets and 500 nm grooved gelatin sheets after 1 h incubation. The shape of the cells on the plane gelatin sheets was round and extended in all directions. SEM images of the cell periphery on the grooved gelatin sheets revealed the extension of several filopodia from the cell in a parallel direction along the inner groove. The grooved pattern seemed to provide a grip for cell adhesion.

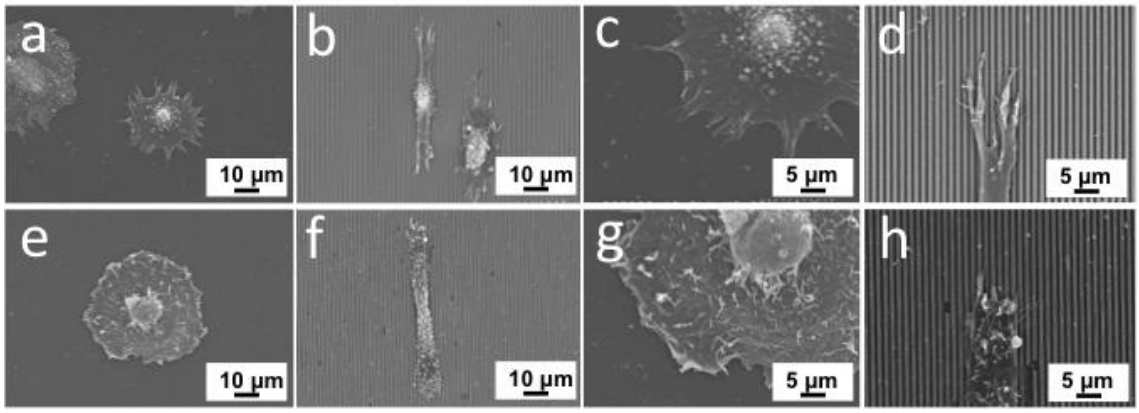

Fig. 7. SEM images of (a-d) human gingival fibroblasts (HGF) and (e-h) human osteoblasts (NHOst) on the grooved gelatin sheet after 1 h incubation. (a, c, e, and g) Plane gelatin sheet (control). (b, d, f, and h) Grooved gelatin sheet with a width of 500 nm and a depth of 500 nm.

4. Discussion

Implant studies have been conducted in various fields to heal and reduce inflammation around implants for new bone ingrowth. Collagen is one of the key proteins in all living tissues; gelatin obtained by irreversible hydrolysis of collagen is used as an anti-hemorrhagic absorbable sponge in surgical operations [27] or a base material for drug delivery capsules [28]. Moreover, collagen/gelatin components have been used for the coating of implant surfaces; surface coating can enhance the initial cell attachment and proliferation of gingival fibroblasts and osteoblasts [6, 7, 10, 12] Therefore, in the present study, we used gelatin in the preparation of micro/nano-grooved sheets for NHOst and HGF assays. The identified behaviors of cell adhesion in this study would contribute toward implant surface modifications that are beneficial for the rapid cell attachment of HGF and NHOst to the implant surface.

Our grooved gelatin sheets prepared via thermal crosslinking had fine structures at the micro/nano level that were similar to the nano-grooved sheets prepared via crosslinking with formaldehyde [17] or 1-ethyl-3-(3-dimethylaminopropyl)carbodiimide hydrochloride (EDC) [18]. Thermal crosslinking can be considered as one of the effective methods for fabrication of fine gelatin patterns at the micro/nano-scale. Furthermore, our patterned gelatin sheets did not use crosslinking agents and thus would not have strong toxicity [29]. Although our patterned gelatin sheets can retain their pattern shape in the culture medium up to a few weeks, the gelatin grooves gradually swelled and became softer (data not shown). The physical strength of the patterned gelatin sheets was sufficiently strong for cell adhesion assay. One limitation of this study was that part of the gelatin was slightly brown colored and degraded from the thermal crosslinking process. In the future, we will develop a fabrication method for the patterned gelatin sheets using mild patterning conditions or/and by crosslinking with biocompatible agents.

The present results demonstrated that the adhesion of NHOst and HGF to gelatin sheets was influenced by the micro/nano-grooves. Our grooved gelatin sheets promoted the initial adhesion of both cell types to the gelatin surface. The results showed that the number of attached cells on the grooved gelatin sheets was about 1.5-1.7 times higher than that of those on the plane gelatin sheets (Fig. 5). However, there are limited reports on cell adhesion assays using NHOst or HGF and grooved collagen/gelatin sheets with a similar groove width range; thus, it is difficult to accurately compare our results with others that have the same conditions. In comparison with adhesion assays that have different groove widths and different cell types, our increased adherent cell number contradicts results that showed decreased cell number on grooved collagen with C2C12 skeletal myoblasts [22]. In comparison with other grooved materials without collagen/gelatin, the increasing number of NHOst on the gelatin groove sheet is in agreement with the results from using grooved plastic film with 1 μm widths after 24 h [30]. However, cell number on the grooved polystyrene with 500 nm widths and 50 nm depths was increased compared with that on the plane sheet, and it was similar to that on the grooved polystyrene with

500 nm widths and 150 nm depths after 1 h [31]. This indicates that groove size and depth can influence cell adhesion. On the other hand, the cell number of HGF on the grooved substrate was more than that on the plane substrate. This is in agreement with other results that use titanium grooves with widths of 100 to 300 nm after 16 h [32], titanium grooves with widths of 15, 30, and 60 μm after 1 h [33], and epoxy grooves with widths of 30 μm after 2 h [34]. These data suggest that cell type and groove size or depth would be important factors of cell adhesion. Alternatively, differences in cell adhesion could be attributed to grooves fabricated by different crosslinking methods. Therefore, our grooved gelatin sheets prepared by thermal crosslinking can promote the cell adhesion of both HGF and NHOst.

Cells on micro/nano-grooves exhibited strong contact guidance and clear alignment along the gelatin groove direction, while cells on a flat surface showed random distribution. Many studies have reported well-aligned cells on the grooved collagen/gelatin sheets. These well-aligned cells were observed with cells such as fibroblasts [15, 17], muscle cells [15, 22], and osteoblasts [24]. Li *et al.* reported that NIH/3T3 cells showed strong cell elongation and faster cell adhesion and growth on a nano-grooved gelatin sheet of 400 nm pitch than on a flat gelatin sheet [17]. Interestingly, endothelial cells were not well-aligned on the nano-grooved gelatin sheet. Zorlutuna *et al.* reported that nano-grooves with widths of 333 nm to 650 nm did not affect endothelial cell proliferation and had a minimal effect on cell alignment [18]. These studies indicate that cell type influences the efficiency of cell alignment. Furthermore, the depth, shape, and size of grooves are expected to affect the degree or angle of cell alignment along the grooves. In our study, both cell types were easily aligned along the grooves because our gelatin patterns have adequate groove widths and because the cells have good cell alignment capability.

Currently, modifications of the micro/nano-architecture of the implant surface have been investigated to minimize clinical problems and promote osteointegration. Prodanov *et al.* reported that when titanium discs with nano-grooves were implanted in rabbit tibia cortical bone, the 300 nm grooved discs showed higher bone-to-implant contact than the conventional blasted and etched titanium discs; nano-grooves on the titanium implant induced earlier bone remodeling [8]. Alternatively, micro/nano-structures of surfaces resembling bone tissue structure may function as hierarchical biomimetic surfaces. Ogawa *et al.* reported that the hierarchical micro/nano-structures of a titanium surface with micro-pits and nano-nodules morphology exhibited greater topographical roughness; in animal models of the implants, the strength of bone-titanium integration was greater for the implants with micro-pits and nano-nodules than for the implants with micro-pits alone [35, 36]. Therefore, the bone-titanium integration could enhance hierarchical micro/nano-structured implants. Depending on the design of implant surface structure, micro/nano-structures and/or patterns on the titanium surface can be a very promising tool to direct bone response at the interface between an implant and the bone tissue. In the future, we plan to fabricate hierarchical micro/nano-structures of collagen/gelatin using our patterning method.

An antibacterial function can be added to the implant surface to prevent peri-implant inflammation from occurring around the gingiva and implant. In our results, the rapid adhesion of NHOst and HGF to micro/nano-patterned gelatin sheets suggests that these cells could be effective for soft-tissue attachment. The development of a stable permucosal seal may be the simplest long-term protection from peri-implantitis and bone resorption[4)]. For further studies, we will need to perform animal periodontal regeneration testing and bone mineralization assay using micro/nano-patterned gelatin sheets.

5. Conclusions

In this study, we developed micro/nano-grooved gelatin sheets with widths of 500 nm, 1 μm, and 2 μm and a depth of 500 nm by nano-imprinting and thermal cycling. The patterns demonstrated rapid cell adhesion and clear cell alignment along the groove direction for NHOst and HGF. These results suggest that our patterns have adequate groove widths, and both cell types have good cell alignment capability.

The development of a stable permucosal seal may be the simplest long-term protection from peri-implantitis and bone resorption. In our results, the rapid adhesion of NHOst and HGF to the groove sheets may be effective for soft-tissue attachment and protection from bone resorption.

Acknowledgements

This work was funded by JSPS KAKENHI Grant No. 26670829, No. 16H05518, and No. 25463047. The analysis of surface profiles for the different patterns was carried out with a laser microscope at the OPEN FACILITY, Hokkaido University Sousei Hall.

References

[1] A.D. Pye, D.E.A. Lockhart, M.P. Dawson, C.A. Murray, A.J. Smith, J Hosp Infect **72**, 104 (2009).
[2] Y. Shibata, Y. Tanimoto, J Prosthodont Res. **59**, 20 (2015).
[3] M. Degidi, D. Nardi, A. Piattelli, Clin Oral Implants Res. **27**, 694 (2016).
[4] D. Cecchinato, A. Parpaiola, L. J. Lindhe, Clin Oral Implants Res. **25**, 791 (2014).
[5] P.A. Jr. Norowski, J.D. Bumgardner, J Biomed Mater Res B Appl Biomater **88**, 530 (2009).
[6] E. Ercan, C. Candirli, T. Arin, L. Kara, C. Uysal, Lasers Med Sci **30**, 11 (2015).
[7] G.E. Pecora, R. Ceccarelli, M. Bonelli, H. Alexander, JL. Ricci, Implant Dent **18**, 57 (2009).
[8] L. Prodanov, E. Lamers, M. Domanski, R. Luttge, JA. Jansen, XF. Walboomers, Biomaterials **34**, 2920 (2013).
[9] K. Gelse, E. Pöschl, T. Aigner, Adv Drug Deliv Rev **55**, 1531 (2003).
[10] M. Nagai, T. Hayakawa, A. Fukatsu, M. Yamamoto, M. Fukumoto, F. Nagahama, H. Mishima, M. Yoshinari, K. Nemoto, T. Kato, Dent Mater J **21**, 250 (2002).
[11] G. Tan, L. Zhou, C. Ning, Y. Tan, G. Ni, J. Liao, P. Yu, X. Chen, Appl Surf Sci **279**, 293 (2013).
[12] Y. Raita, K. Komatsu, T. Hayamawa, Dent Mater J **34**, 847 (2015).
[13] K. Yue, G. Trujillo-de Santiago, MM. Alvarez, A. Tamayol, N. Annabi, A. Khademhosseini, Biomaterials **73**, 254 (2015).
[14] J. Yoo, M. Noh, H. Kim, N.L. Jeon, B.S. Kim, J. Kim, Biomaterials **45**, 36 (2015).
[15] R.B. Vernon, M.D. Gooden, S.L. Lara, T.N. Wight, Biomaterials **26**, 3131 (2005).
[16] Y.C. Ou, C.W. Hsu, L.J. Yang, H.C. Han, Y.W. Liu, C.Y. Chen, Sensor Mater **20**, 435 (2008).
[17] S.S. Li, J. Shi, L. Liu, JJ. Li, LM. Jiang, CX. Luo, K. Kamei, Y. Chen, Microelectron Eng **110**, 70 (2013).
[18] P. Zorlutuna, Z. Rong, P. Vadgama, V. Hasirci, Acta Biomater **5**, 2451 (2009).
[19] A. Islam, K. Chapin, M. Younesi, O. Akkus, Biofabrication **7**, 035005 (2015).
[20] R. Gruschwitz, J. Friedrichs, M. Valtink, CM. Franz, Dj. Müller, RH. Funk, K. Engelmann, Invest Ophthalmol Vis Sci. **51**, 6303 (2010).
[21] ML. McCain, A. Agarwal, HW. Nesmith, AP. Nesmith, KK. Parker, Biomaterials **35**, 5462 (2014).
[22] S. Chen, S. Chinnathambi, X. Shi, A. Osaka, Y. Zhu, N. Hanagata, J Mater Chem **22**, 21885 (2012).
[23] GD. Pins, M. Toner, JR. Morgan, FASEB J **14**, 593 (2000).
[24] S. Ber, G. Torun Köse, V. Hasirci, Biomaterials **26**, 1977 (2005).
[25] T. Akasaka, A. Yokoyama, M. Matsuoka, T. Hashimoto, S. Abe, M. Uo, F. Watari, Biomed Mater Eng **19**, 147 (2009).
[26] W. Tsai, Y. Ting, J. Yang, J. Lai, H. Liu, J Mater Sci **20**, 1367 (2009).
[27] JP**.** Draye, B. Delaey, A. Van de Voorde, A. Van Den Bulcke, B. De Reu, E. Schacht, Biomaterials **19**, 16771 (998).
[28] V. DiTizio, C. Karlgard, L. Lilge, E. Antoine, AE. Khoury, MW. Mittelman, F. DiCosmo, J Biomed Mater Res **51**, 96 (2000).
[29] H. Tsujimoto, A. Tanzawa, H. Miyamoto, T. Horii, M. Tsuji, A. Kawasumi, A. Tamura, Z. Wang, R. Abe, S. Tanaka, K. Yamanaka, M. Matoba, H. Torii, Y. Ozamoto, H. Takamori, S. Suzuki, S. Morita, Y. Ikada, A. Hagiwara, J Biomed Mater Res B Appl Biomater **103**, 1511 (2015).
[30] H. Kenar, A. Kocabas, A. Aydinli, V. Hasirci. J Biomed Mater Res A **85**, 1001 (2008).
[31] S. Lenhert, MB. Meier, U. Meyer, L. Chi, HP. Wiesmann, Biomaterials **26,** 563 (2005).
[32] BJ. Im, SW. Lee, N. Oh, MH. Lee, JH. Kang, R. Leesungbok, SC. Lee, SJ. Ahn, JS. Park, Arch Oral Biol **57**, 898 (2012).

[33] SW. Lee, SY. Kim, IC. Rhyu, WY. Chung, R. Leesungbok, KW. Lee, Clin Oral Implants Res **20**, 56 (2009).
[34] E. Kokubu, DW. Hamilton, T. Inoue, DM. Brunette, J Biomed Mater Res A **91**, 663 (2009).
[35] K. Kubo, N. Tsukimura, F. Iwasa, T. Ueno, L. Saruwatari, H. Aita, WA. Chiou, T. Ogawa, Biomaterials **30**, 5319 (2009).
[36] T. Ogawa, L. Saruwatari, K. Takeuchi, H. Aita, N. Ohno, J Dent Res **87**, 751 (2008).